

Study of Influence of an Overhead Ground Wire on Electric Fields around the HV Power Transmission Line Using 2D and 3D Finite Element Method

P. PAO-LA-OR*, A. ISARAMONGKOLRAK, and T. KULWORAWANICHPONG

Power System Research Unit, School of Electrical Engineering
Institute of Engineering, Suranaree University of Technology
111 University Avenue, Muang District, Nakhon Ratchasima, 30000
THAILAND

*Corresponding author: padej@sut.ac.th

Abstract: - This paper has proposed a mathematical model of electric fields caused by high voltage conductors of electric power transmission systems by using a set of second-order partial differential equations. This study has considered the effect of the overhead ground wire on electric fields emitted around the high voltage transmission line. Comparison among two test cases, with and without the overhead ground wire, has been illustrated. Computer-based simulation utilizing the two-dimensional (2D) and three-dimensional (3D) finite element method in the time harmonic mode, instructed in MATLAB programming environment with graphical representation for electric field strength has been investigated. The simulation results show that the transmission system having the overhead ground wire can remarkably reduced the intensity of the electric field strength.

Key-Words: - Overhead Ground Wire (OHGW), Electric Field Strength, Finite Element Method (FEM), Transmission Line, Computer Simulation

1 Introduction

An overhead ground wire (OHGW) is one of key components in electrical power transmission systems. It is a small metal conductor run between the tops of overhead power transmission towers. At each tower, the OHGW is connected to ground through the tower metal frame. It exhibits the protection of high voltage conductors from lightning strokes. Beside the lightning protection, the OHGW also influences electric field distribution around the power transmission lines caused by the high voltage conductors. Finite Element Method (FEM) is one of the most popular numerical methods used for computer simulation. The key advantage of the FEM over other numerical methods in engineering applications is the ability to handle nonlinear, time-dependent and circular geometry problems. Therefore, this method is suitable for solving the problem involving electric field effects around the transmission line caused by circular cross-section of high voltage conductors. Especially, when the transmission length is taken into account, the region domain is three-dimensional.

From literature, most research works involving the OHGW mainly devote to put emphasis on reducing the effects of lightning strokes on overhead transmission lines [1-3]. In this paper, the study on the OHGW resulting in electric field distribution around the transmission line is proposed. A 115-kV

power transmission line of Provincial Electricity Authority (PEA) in Nakhon Ratchasima province hung over a 22-kV power distribution line on the same tower is selected for test. The computer simulation based on the 2D and 3D-FEM in the time harmonic mode with appropriate graphical representation of electric fields is conducted.

2 Modeling of Electric Fields involving Electric Power Transmission Lines

A mathematical model of electric fields (\mathbf{E}) radiating around a transmission line is usually expressed in the wave equation (Helmholtz's equation) as Eq.(1) [4-5] derived from Faraday's law.

$$\nabla^2 \mathbf{E} - \sigma \mu \frac{\partial \mathbf{E}}{\partial t} - \varepsilon \mu \frac{\partial^2 \mathbf{E}}{\partial t^2} = 0 \quad (1)$$

..., where ε is the dielectric permittivity of media, μ and σ are the magnetic permeability and the conductivity of conductors, respectively.

This paper has considered the system governing by using the time harmonic mode and representing the electric field in complex form, $\mathbf{E} = E e^{j\omega t}$ [6], therefore,

$$\frac{\partial \mathbf{E}}{\partial t} = j\omega \mathbf{E} \quad \text{and} \quad \frac{\partial^2 \mathbf{E}}{\partial t^2} = -\omega^2 \mathbf{E}$$

..., where ω is the angular frequency.

From Eq.(1), by substituting the complex electric field, Eq.(1) can be transformed to an alternative form as follows.

$$\nabla^2 E - j\omega\sigma\mu E + \omega^2 \varepsilon\mu E = 0$$

When considering the problem of 2D in Cartesian coordinate (x,y) , hence

$$\frac{\partial}{\partial x} \left(\frac{1}{\mu} \frac{\partial E}{\partial x} \right) + \frac{\partial}{\partial y} \left(\frac{1}{\mu} \frac{\partial E}{\partial y} \right) - (j\omega\sigma - \omega^2 \varepsilon) E = 0 \quad (2)$$

In the similar manner, when considering the problem of 3D in Cartesian coordinate (x,y,z) , (2) can be rewritten as follows.

$$\frac{\partial}{\partial x} \left(\frac{1}{\mu} \frac{\partial E}{\partial x} \right) + \frac{\partial}{\partial y} \left(\frac{1}{\mu} \frac{\partial E}{\partial y} \right) + \frac{\partial}{\partial z} \left(\frac{1}{\mu} \frac{\partial E}{\partial z} \right) - (j\omega\sigma - \omega^2 \varepsilon) E = 0 \quad (3)$$

Analytically, there is no simple exact solution of the above equation. Therefore, in this paper the FEM is chosen to be a potential tool for finding approximate electric field solutions for the PDE described in Eq.(2) and Eq.(3) [7-9].

3 System Description with the FEM

3.1 Discretization

This paper conducts the simulation study by considering the 115-kV PEA's transmission system in Nakhon Ratchasima province. This type of power transmission systems is common in rural areas in Thailand. The selected test system consists of 2-bundle conductors configuring in vertical conductor arrangement as shown in Fig. 1. Also, a 22-kV power line in horizontal conductor arrangement is hung below the HV transmission line. Fig. 2 depicts the detail of the test system.

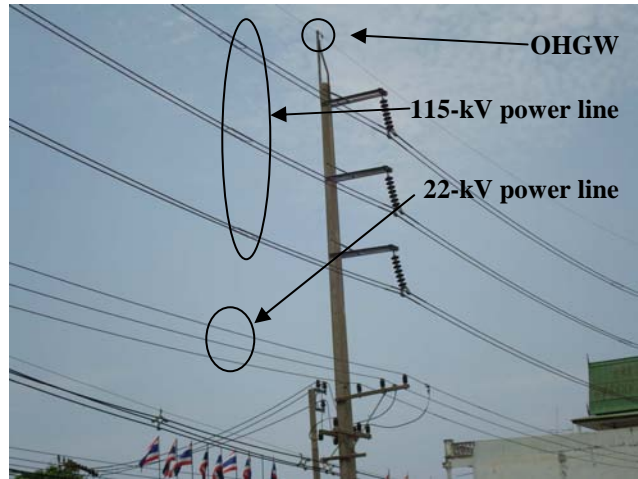


Fig.1 Case study in Nakhon Ratchasima province

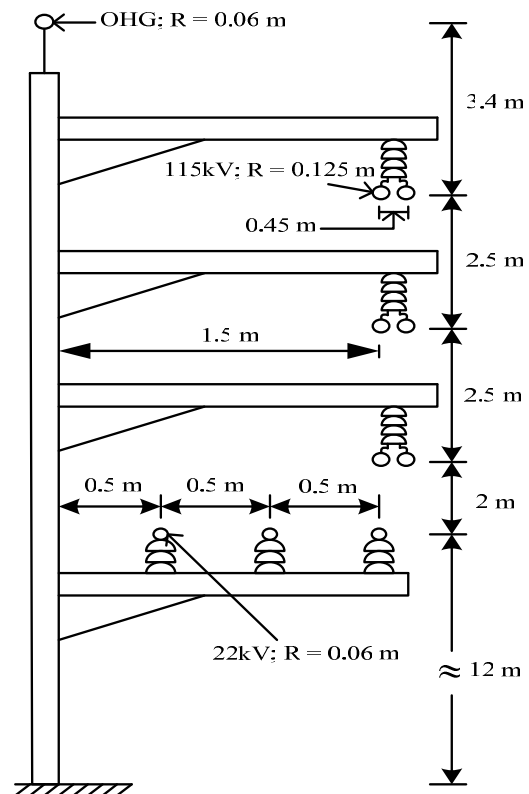


Fig.2 Detail of the test system

The domain of study with the 2D-FEM can be discretized by using linear triangular elements. Fig. 3 and 4 show grid representation of the test system with and without the OHGW, respectively. For Fig. 3, with the appearance of the OHGW, the region domain consists of 1896 nodes and 3751 elements, while in Fig. 4, where the OHGW is not included, the system has the total number of 1391 nodes and 2745 elements. Fig. 5 is just a zoom-in version of Fig. 4 to show how triangular meshes around the conductors are generated.

Also, the domain of study with the 3D-FEM can be discretized by using linear tetrahedron elements. Fig. 6 and 7 show grid representation of the test system with and without the OHGW, respectively. From these figures, a 20-m transmission-line portion of which 115-kV and 22-kV systems is straight and line tension sags are not assumed. For Fig. 6, with the appearance of the OHGW, the region domain consists of 3761 nodes and 21785 elements, while in Fig. 7, where the OHGW is not included, the system has the total number of 3551 nodes and 19271 elements. Fig. 8 is just a zoom-in version of Fig. 7 to show how 3D meshes of the conductors are generated.

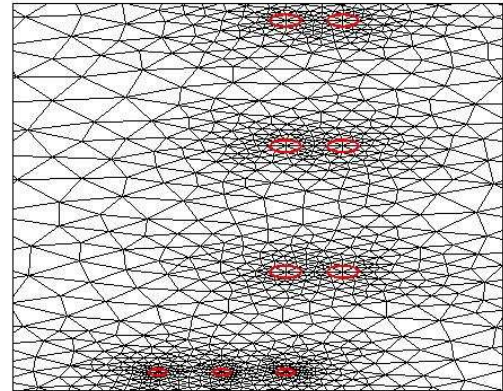


Fig.5 2D grid around the conductors

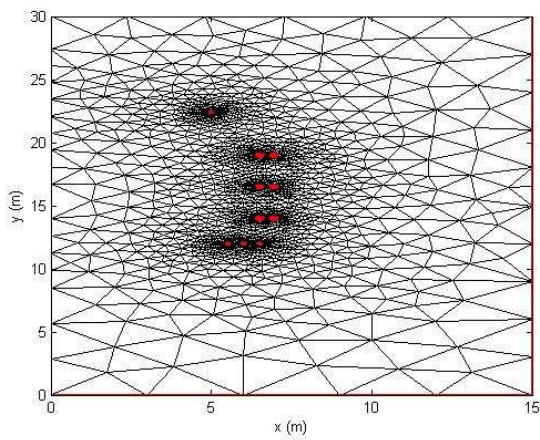


Fig.3 2D test system with the OHGW

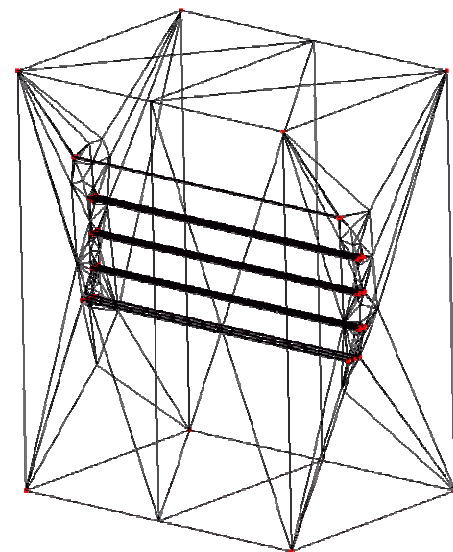


Fig.6 3D test system with the OHGW

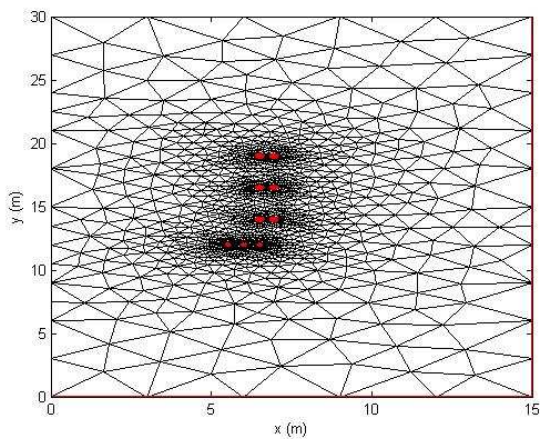


Fig.4 2D test system without the OHGW

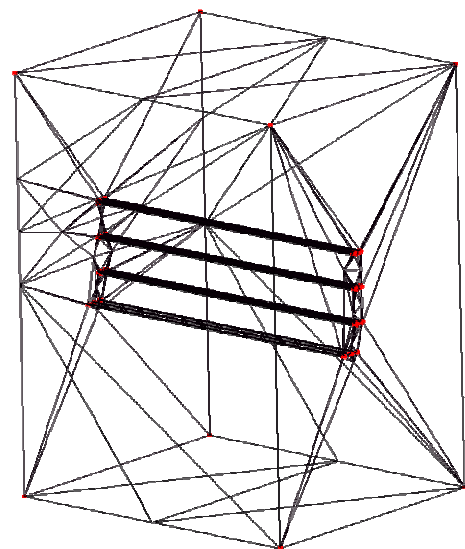


Fig.7 3D test system without the OHGW

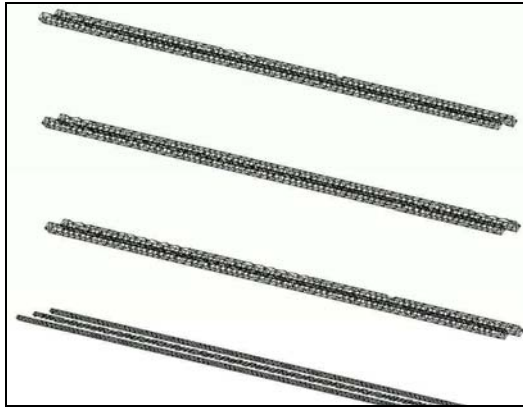


Fig.8 3D meshed of the conductors

3.2 Finite Element Formulation

An equation governing each element is derived from the Maxwell's equations directly by using Galerkin approach, which is the particular weighted residual method for which the weighting functions are the same as the shape function. However, the shape function used for 2D and 3D problems is different.

3.2.1 2D-FEM Formulation

The shape function for 2D-FEM used in this research is the application of 3-node triangular element (two-dimensional linear element) [10-11]. According to the method, the electric field is expressed as follows.

$$E(x, y) = E_i N_i + E_j N_j + E_k N_k \quad (4)$$

..., where N_n , $n = i, j, k$ is the element shape function and the E_n , $n = i, j, k$ is the approximation of the electric field at each node (i, j, k) of the elements, which is

$$N_n = \frac{a_n + b_n x + c_n y}{2\Delta_e}$$

..., where Δ_e is the area of the triangular element and,

$$\begin{aligned} a_i &= x_j y_k - x_k y_j, & b_i &= y_j - y_k, & c_i &= x_k - x_j \\ a_j &= x_k y_i - x_i y_k, & b_j &= y_k - y_i, & c_j &= x_i - x_k \\ a_k &= x_i y_j - x_j y_i, & b_k &= y_i - y_j, & c_k &= x_j - x_i. \end{aligned}$$

The method of the weighted residue with Galerkin approach is then applied to the differential equation, Eq.(2), where the integrations are performed over the element domain Ω .

$$\int_{\Omega} N_n \left(\frac{\partial}{\partial x} \left(\frac{1}{\mu} \frac{\partial E}{\partial x} \right) + \frac{\partial}{\partial y} \left(\frac{1}{\mu} \frac{\partial E}{\partial y} \right) \right) d\Omega - \int_{\Omega} N_n (j\omega\sigma - \omega^2 \varepsilon) E d\Omega = 0$$

, or in the compact matrix form

$$[M + K]\{E\} = 0 \quad (5)$$

$$M = (j\omega\sigma - \omega^2 \varepsilon) \int_{\Omega} N_n N_m d\Omega$$

$$= \frac{(j\omega\sigma - \omega^2 \varepsilon) \Delta_e}{12} \begin{bmatrix} 2 & 1 & 1 \\ 1 & 2 & 1 \\ 1 & 1 & 2 \end{bmatrix}$$

$$\begin{aligned} K &= \nu \int_{\Omega} \left(\frac{\partial N_n}{\partial x} \frac{\partial N_m}{\partial x} + \frac{\partial N_n}{\partial y} \frac{\partial N_m}{\partial y} \right) d\Omega \\ &= \frac{\nu}{4\Delta_e} \begin{bmatrix} b_i b_i + c_i c_i & b_i b_j + c_i c_j & b_i b_k + c_i c_k \\ & b_j b_j + c_j c_j & b_j b_k + c_j c_k \\ Sym & & b_k b_k + c_k c_k \end{bmatrix} \end{aligned}$$

..., where ν is the material reluctivity ($\nu = 1/\mu$).

For one element containing 3 nodes, the expression of the FEM approximation is a 3×3 matrix. With the account of all elements in the system of n nodes, the system equation is sizable as the $n \times n$ matrix.

3.2.2 3D-FEM Formulation

The shape function for 3D-FEM used in this research is the application of 4-node tetrahedron element (three-dimensional linear element) [12-14]. According to the method, the electric field is expressed as follows.

$$E(x, y, z) = E_1 N_1 + E_2 N_2 + E_3 N_3 + E_4 N_4 \quad (6)$$

..., where N_i , $i = 1, 2, 3, 4$ is the element shape function and the E_i , $i = 1, 2, 3, 4$ is the approximation of the electric field at each node (1, 2, 3, 4) of the elements, which is

$$N_i = \frac{1}{6V} (a_i + b_i x + c_i y + d_i z)$$

..., where V is the volume of the tetrahedron element, which is expressed as

$$V = \frac{1}{6} \begin{bmatrix} 1 & x_1 & y_1 & z_1 \\ 1 & x_2 & y_2 & z_2 \\ 1 & x_3 & y_3 & z_3 \\ 1 & x_4 & y_4 & z_4 \end{bmatrix}$$

and

$$\begin{aligned} a_1 &= x_4(y_2z_3 - y_3z_2) + x_3(y_4z_2 - y_2z_4) + x_2(y_3z_4 - y_4z_3) \\ a_2 &= x_4(y_3z_1 - y_1z_3) + x_3(y_1z_4 - y_4z_1) + x_1(y_4z_3 - y_3z_4) \\ a_3 &= x_4(y_1z_2 - y_2z_1) + x_2(y_4z_1 - y_1z_4) + x_1(y_2z_4 - y_4z_2) \\ a_4 &= x_3(y_2z_1 - y_1z_2) + x_2(y_1z_3 - y_3z_1) + x_1(y_3z_2 - y_2z_3) \end{aligned}$$

$$\begin{aligned} b_1 &= y_4(z_3 - z_2) + y_3(z_2 - z_4) + y_2(z_4 - z_3) \\ b_2 &= y_4(z_1 - z_3) + y_1(z_3 - z_4) + y_3(z_4 - z_1) \\ b_3 &= y_4(z_2 - z_1) + y_2(z_1 - z_4) + y_1(z_4 - z_2) \\ b_4 &= y_3(z_1 - z_2) + y_1(z_2 - z_3) + y_2(z_3 - z_1) \end{aligned}$$

$$\begin{aligned} c_1 &= x_4(z_2 - z_3) + x_2(z_3 - z_4) + x_3(z_4 - z_2) \\ c_2 &= x_4(z_3 - z_1) + x_3(z_1 - z_4) + x_1(z_4 - z_3) \\ c_3 &= x_4(z_1 - z_2) + x_1(z_2 - z_4) + x_2(z_4 - z_1) \\ c_4 &= x_3(z_2 - z_1) + x_2(z_1 - z_3) + x_1(z_3 - z_2) \end{aligned}$$

$$\begin{aligned} d_1 &= x_4(y_3 - y_2) + x_3(y_2 - y_4) + x_2(y_4 - y_3) \\ d_2 &= x_4(y_1 - y_3) + x_1(y_3 - y_4) + x_3(y_4 - y_1) \\ d_3 &= x_4(y_2 - y_1) + x_2(y_1 - y_4) + x_1(y_4 - y_2) \\ d_4 &= x_3(y_1 - y_2) + x_1(y_2 - y_3) + x_2(y_3 - y_1) \end{aligned}$$

The method of the weighted residue with Galerkin approach is then applied to the differential equation, Eq.(3), where the integrations are performed over the element domain Ω .

$$\int_{\Omega} N_i \left(\frac{\partial}{\partial x} \left(\frac{1}{\mu} \frac{\partial E}{\partial x} \right) + \frac{\partial}{\partial y} \left(\frac{1}{\mu} \frac{\partial E}{\partial y} \right) + \frac{\partial}{\partial z} \left(\frac{1}{\mu} \frac{\partial E}{\partial z} \right) \right) d\Omega - \int_{\Omega} N_i (j\omega\sigma - \omega^2\varepsilon) E d\Omega = 0$$

, or in the compact matrix form

$$[M + K]\{E\} = 0$$

$$\begin{aligned} M &= (j\omega\sigma - \omega^2\varepsilon) \int_{\Omega} N_i N_j d\Omega \\ &= \frac{(j\omega\sigma - \omega^2\varepsilon)V}{20} \begin{bmatrix} 2 & 1 & 1 & 1 \\ 1 & 2 & 1 & 1 \\ 1 & 1 & 2 & 1 \\ 1 & 1 & 1 & 2 \end{bmatrix} \end{aligned}$$

$$\begin{aligned} K &= \nu \int_{\Omega} \left(\frac{\partial N_i}{\partial x} \frac{\partial N_j}{\partial x} + \frac{\partial N_i}{\partial y} \frac{\partial N_j}{\partial y} + \frac{\partial N_i}{\partial z} \frac{\partial N_j}{\partial z} \right) d\Omega \\ &= \frac{\nu}{36V} \begin{bmatrix} b_1b_1 + c_1c_1 + d_1d_1 & b_1b_2 + c_1c_2 + d_1d_2 \\ b_1b_2 + c_1c_2 + d_1d_2 & b_2b_2 + c_2c_2 + d_2d_2 \\ b_1b_3 + c_1c_3 + d_1d_3 & b_2b_3 + c_2c_3 + d_2d_3 \\ b_1b_4 + c_1c_4 + d_1d_4 & b_2b_4 + c_2c_4 + d_2d_4 \\ b_1b_3 + c_1c_3 + d_1d_3 & b_1b_4 + c_1c_4 + d_1d_4 \\ b_2b_3 + c_2c_3 + d_2d_3 & b_2b_4 + c_2c_4 + d_2d_4 \\ b_3b_3 + c_3c_3 + d_3d_3 & b_3b_4 + c_3c_4 + d_3d_4 \\ b_3b_4 + c_3c_4 + d_3d_4 & b_4b_4 + c_4c_4 + d_4d_4 \end{bmatrix} \end{aligned}$$

For one element containing 4 nodes, the expression of the FEM approximation is a 4x4 matrix. With the account of all elements in the system of n nodes, the system equation is sizable as the $n \times n$ matrix.

3.3 Boundary Conditions and Simulation Parameters

The boundary conditions applied here are that to set zero electric fields at the ground level and the OHGW. In addition, the boundary condition of conductor surface in both 115-kV and 22-kV power lines are assigned as given in [15-16]. This simulation uses the system frequency of 50 Hz. Both power lines are bared conductors of Aluminum Conductor Steel Reinforced (ACSR), having the conductivity (σ) = 0.8×10^7 S/m, the relative permeability (μ_r) = 300, the relative permittivity (ε_r) = 3.5. It notes that the free space permeability (μ_0) is $4\pi \times 10^{-7}$ H/m, and the free space permittivity (ε_0) is 8.854×10^{-12} F/m [17].

4 Results and Discussion

Simulation results obtained by using MATLAB programming for which 2D and 3D-FEM can be simulated, numerically. Especially, in 2D cases, the

results can be graphically presented in the contour of electric fields dispersed thoroughly the cross-sectional area of study. Fig.9 and Fig.10 illustrate the result of electric field distribution of 2D-FEM for a test case of with and without the OHGW, respectively.

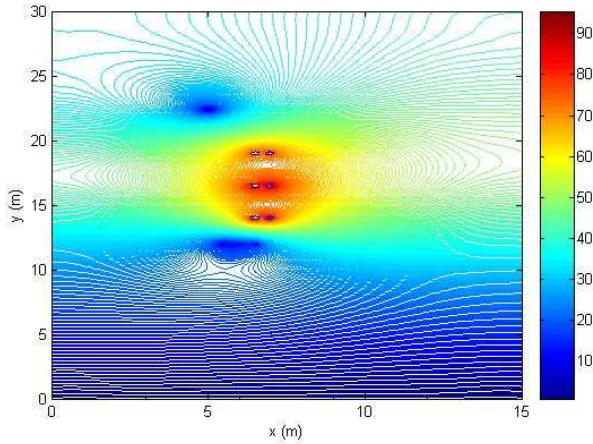


Fig.9 Contour of the electric field (kV/m) with the OHGW

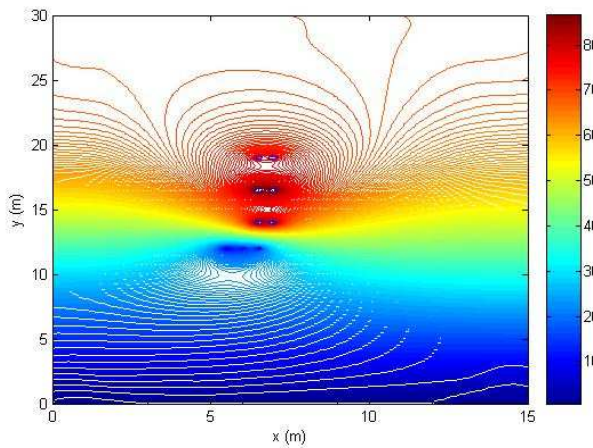


Fig.10 Contour of the electric field (kV/m) without the OHGW

For which 3D-FEM results, those can be graphically presented in the filled polygon of electric fields dispersed thoroughly the volume of study. Fig.11 and Fig.12 illustrate the result of electric field distribution of 3D-FEM for a test case of with and without the OHGW, respectively. Fig.13 and Fig.14 reveal that electric field distribution around the conductor surfaces for the case with the OHGW is considerably reduced in their valued when compared with those of the same position of the case without the OHGW.

For the OHGW case, Fig.15 – 19 illustrate results of electric field contours on the cross-sectional area perpendicular to the z axis, where the cutaway

positions are given at z = 0, 5, 10, 15 and 20 m, respectively. For the case without the OHGW, Fig.20 – 24 illustrate results of electric field contours as described for the case of the OHGW.

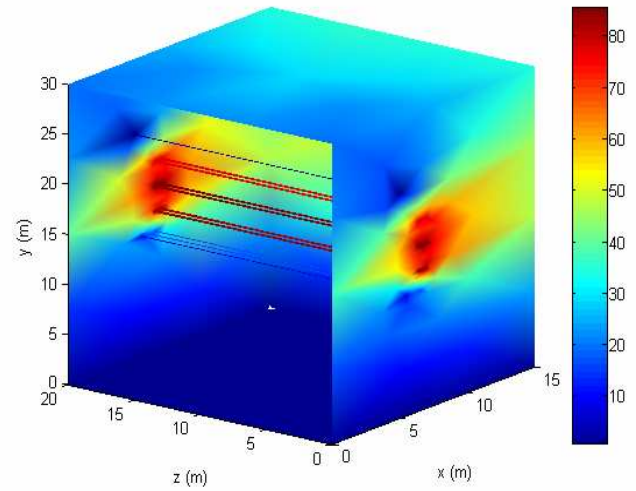


Fig.11 Electric field (kV/m) of the region domain for the OHGW case

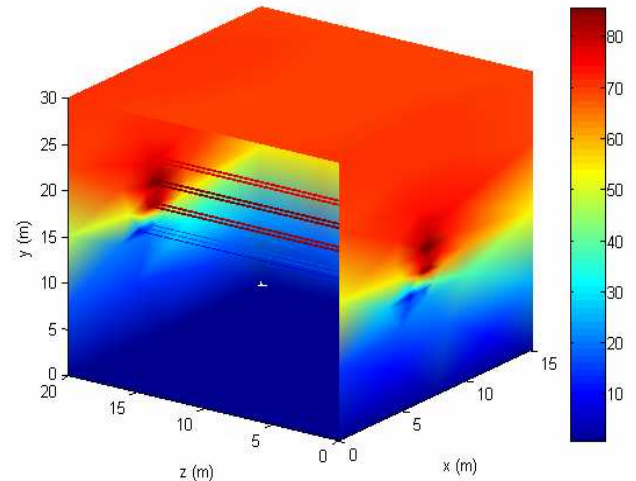


Fig.12 Electric field (kV/m) of the region domain for the case without the OHGW

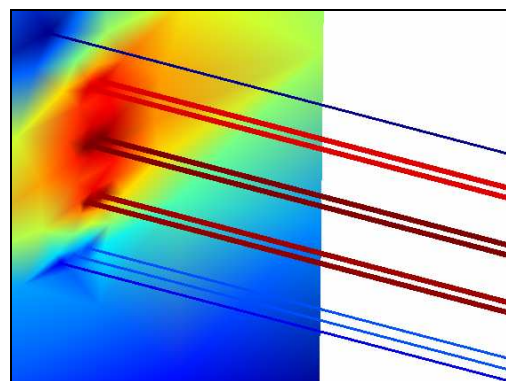


Fig.13 Electric field (kV/m) around the conductor space for the OHGW case

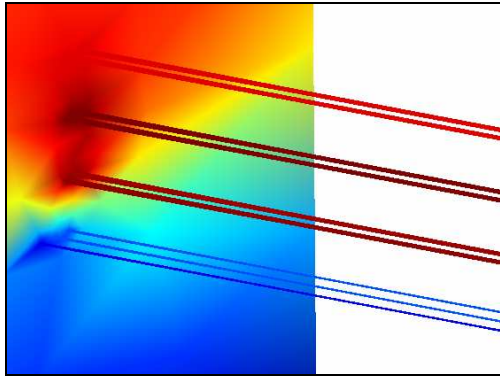


Fig.14 Electric field (kV/m) around the conductor space for the case without the OHGW

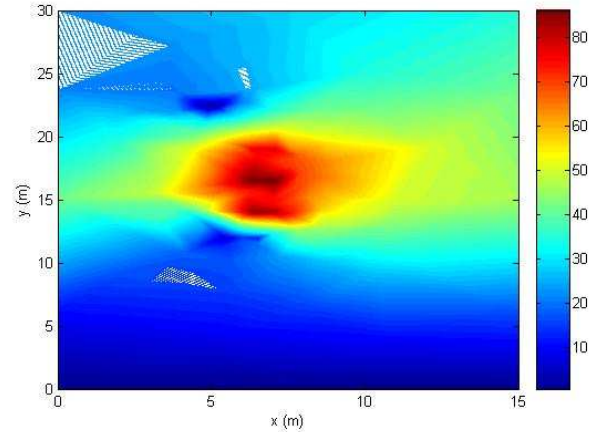


Fig.17 Electric field contour (kV/m) at a cutaway position of 10 m for the OHGW case

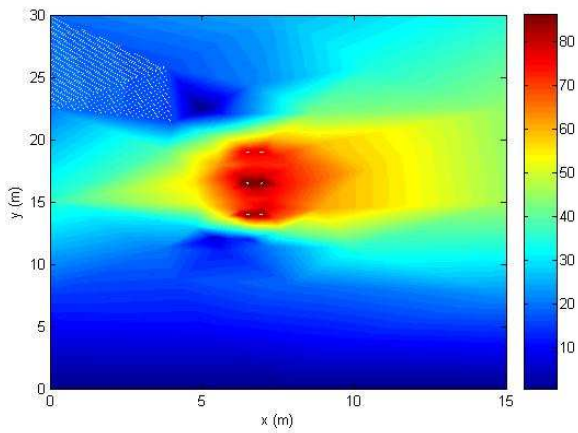


Fig.15 Electric field contour (kV/m) at a cutaway position of 0 m for the OHGW case

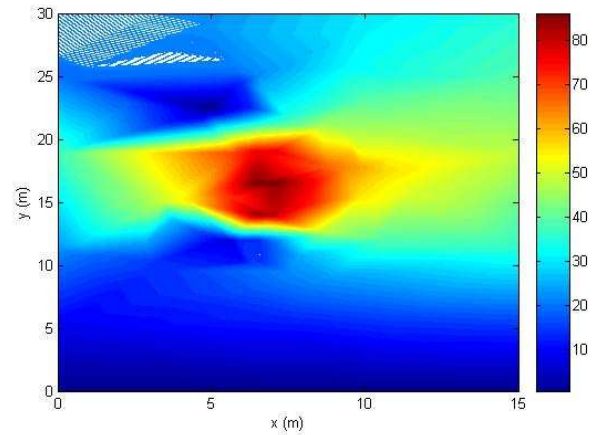


Fig.18 Electric field contour (kV/m) at a cutaway position of 15 m for the OHGW case

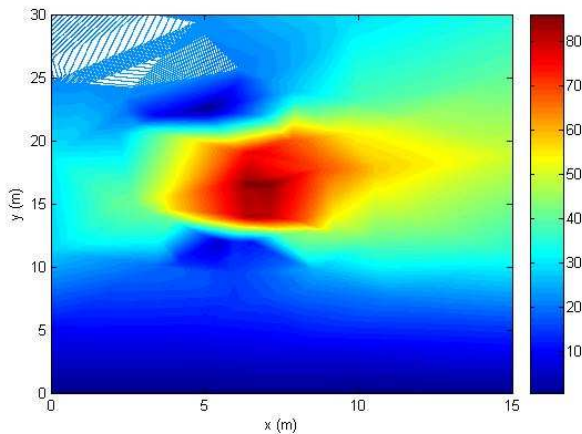


Fig.16 Electric field contour (kV/m) at a cutaway position of 5 m for the OHGW case

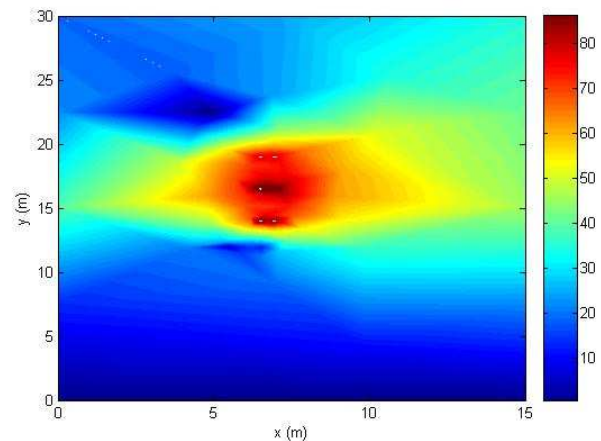


Fig.19 Electric field contour (kV/m) at a cutaway position of 20 m for the OHGW case

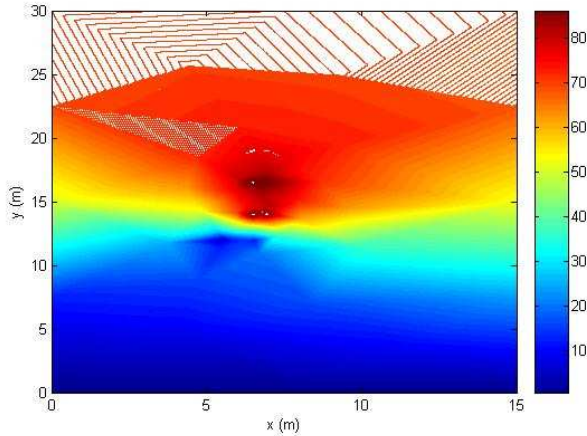


Fig.20 Electric field contour (kV/m) at a cutaway position of 0 m for the case without the OHGW

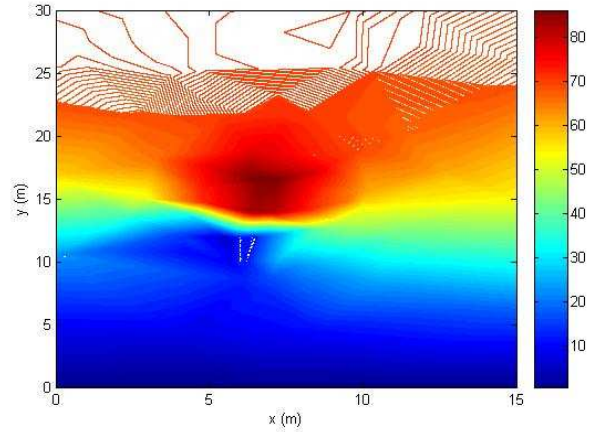


Fig.23 Electric field contour (kV/m) at a cutaway position of 15 m for the case without the OHGW

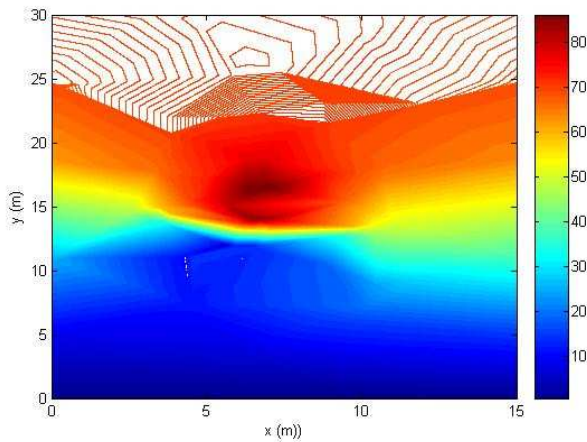


Fig.21 Electric field contour (kV/m) at a cutaway position of 5 m for the case without the OHGW

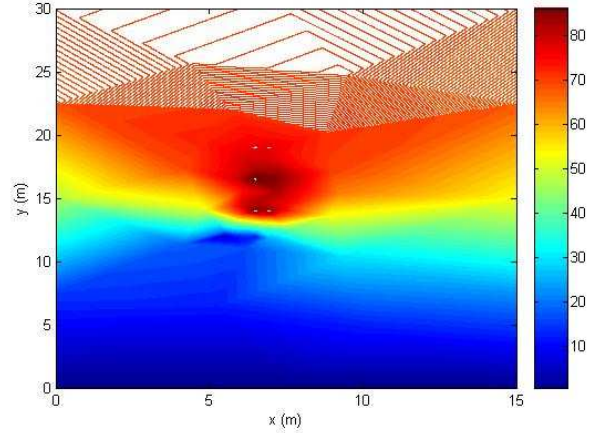


Fig.24 Electric field contour (kV/m) at a cutaway position of 20 m for the case without the OHGW

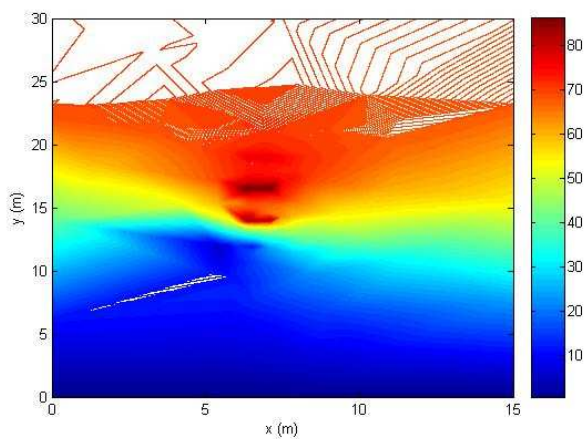


Fig.22 Electric field contour (kV/m) at a cutaway position of 10 m for the case without the OHGW

The illustrative electric field contours show that the amplitude of the electric field with the OHGW tied at the top of the tower is lower than that of the case without the OHGW. By investigating closer at the height of 1.0-m above the ground ($y = 1.0\text{-m}$), results of which 2D and 3D-FEM cases are put in Table 1. From those results, the average electric field magnitude is significantly reduced by 10% for both 2D and 3D calculations. For the 2D-FEM, $(3.0777-2.7304)/3.0777 = 11.28\%$ and, for the 3D-FEM, $(2.8487-2.4986)/2.8487 = 12.29\%$, resulting from placing the OHGW at the top of the tower. Table 2 illustrates the average of electric fields for both cases at some specific height level above the ground for comparison.

Table 1 Comparison of electric field distribution (kV/m) at $y = 1.0$ -m above the ground

x (m)	2D-FEM		3D-FEM	
	With OHGW	Without OHGW	With OHGW	Without OHGW
0	2.6159	2.9923	2.3523	2.6623
1	2.6508	3.0415	2.3624	2.7998
2	2.5596	2.9412	2.2432	2.7543
3	2.5427	2.8964	2.2543	2.6745
4	2.5661	2.8740	2.2448	2.6754
5	2.6066	2.8803	2.3843	2.6832
6	2.6459	2.9410	2.3849	2.6934
7	2.6726	2.9975	2.3926	2.7002
8	2.7002	3.0495	2.4736	2.7069
9	2.7419	3.0966	2.4932	2.8123
10	2.7804	3.1272	2.5511	2.9234
11	2.8125	3.1531	2.7024	2.9476
12	2.8519	3.1953	2.7235	2.9739
13	2.9195	3.2724	2.8012	3.0211
14	3.0249	3.4087	2.8201	3.2825
15	2.9951	3.3768	2.7932	3.2678
Average	2.7304	3.0777	2.4986	2.8487

Table 2 Comparison of the electric field (kV/m) averages at specific height above the ground

y (m)	2D-FEM		3D-FEM	
	With OHGW	Without OHGW	With OHGW	Without OHGW
1	2.7304	3.0777	2.4986	2.8487
5	13.2482	14.8437	12.5620	13.9875
10	26.5636	29.8113	24.7396	28.5248
15	51.7035	59.0658	52.8041	58.5954
20	48.9177	67.6321	46.7814	68.2646
25	38.0124	67.8528	35.7599	69.2985
30	37.9455	67.8902	34.7877	69.3922

5 Conclusion

This paper presents the study on the OHGW resulting in electric field distribution around the electric power transmission line. A 115-kV power transmission line of Provincial Electricity Authority (PEA) in Nakhon Ratchasima province hung over a 22-kV power distribution line on the same tower is selected for test. The computer simulation based on the 2D and 3D-FEM in the time harmonic mode with appropriate graphical representation of electric fields is conducted. As a result, it can conclude that the OHGW has the ability to reduce the electric field intensity caused by high voltage conductors. The percentage reduction approximately varies from

10% - 50%, according on the height level above the ground.

References:

- [1] Yokoya, M., Katsuragi, Y., Goda, Y., Nagata, Y., and Asano, Y., Development of Lightning-resistant Overhead Ground Wire, *IEEE Transactions on Power Delivery*, Vol.9, No.3, 1994, pp. 1517-1523.
- [2] He, J., Tu, Y., Zeng, R., Lee, J.B., Chang, S.H., and Guan, Z., Numeral Analysis Model for Shielding Failure of Transmission Line Under Lightning Stroke, *IEEE Transactions on Power Delivery*, Vol.20, No.2, 2005, pp. 815-822.
- [3] Zeng, R., He, J., Lee, J., Chang, S., Tu, Y., Gao, Y., Zou, J., and Guan, Z., Influence of Overhead Transmission Line on Grounding Impedance Measurement of Substation, *IEEE Transactions on Power Delivery*, Vol.20, No.2, 2005, pp. 1219-1225.
- [4] Chari, M.V.K., and Salon, S.J., *Numerical Methods in Electromagnetism*, Academic Press, USA, 2000.
- [5] Weiner, M., *Electromagnetic Analysis Using Transmission Line Variables*, World Scientific Publishing, Singapore, 2001.
- [6] Christopoulos, C., *The Transmission-Line Modeling Method: TLM*, IEEE Press, USA, 1995.
- [7] Pao-la-or, P., Kulworawanichpong, T., Sujitjorn, S., and Peaiyoung, S., Distributions of Flux and Electromagnetic Force in Induction Motors: A Finite Element Approach, *WSEAS Transactions on Systems*, Vol.5, No.3, 2006, pp. 617-624.
- [8] Pao-la-or, P., Sujitjorn, S., Kulworawanichpong, T., and Peaiyoung, S., Studies of Mechanical Vibrations and Current Harmonics in Induction Motors Using Finite Element Method, *WSEAS Transactions on Systems*, Vol.7, No.3, 2008, pp. 195-202.
- [9] Chen, R.C., An Iterative Method for Finite-Element Solutions of the Nonlinear Poisson-Boltzmann Equation, *WSEAS Transactions on Computers*, Vol.7, No.4, 2008, pp. 165-173.
- [10] Preston, T.W., Reece, A.B.J., and Sangha, P.S., Induction Motor Analysis by Time-Stepping Techniques, *IEEE Transactions on Magnetics*, Vol.24, No.1, 1988, pp. 471-474.
- [11] Kim, B.T., Kwon, B.I., and Park, S.C., Reduction of Electromagnetic Force Harmonics in Asynchronous Traction Motor by Adapting the Rotor Slot Number, *IEEE Transactions on Magnetics*, Vol.35, No.5, 1999, pp. 3742-3744.

- [12] Lewis, R.W., Nithiarasu, P., and Seetharamu, K.N., *Fundamentals of the Finite Element Method for Heat and Fluid Flow*, John Wiley & Sons, USA, 2004.
- [13] Bhatti M.A., *Advanced Topics in Finite Element Analysis of Structures*, John Wiley & Sons, USA, 2006.
- [14] Kattan P.I., *MATLAB Guide to Finite Elements (2nd edition)*, Springer Berlin Heidelberg, USA, 2007.
- [15] Iyyuni, G.B., and Sebo, S.A., Study of Transmission Line Magnetic Fields, *Proceedings of the Twenty-Second Annual North American, IEEE Power Symposium*, 1990, pp. 222-231.
- [16] Pin-anong, P., *The Electromagnetic Field Effects Analysis which Interfere to Environment near the Overhead Transmission Lines and Case Study of Effects Reduction*, [M.Eng. thesis], School of Electrical Engineering, Department of Electrical Engineering, King Mongkut's Institute of Technology Ladkrabang, Bangkok, Thailand, 2002.
- [17] Hayt, Jr.W.H., and Buck, J.A., *Engineering Electromagnetics (7th edition)*, McGraw-Hill, Singapore, 2006.